

INFORMATION TO USERS

This reproduction was made from a copy of a document sent to us for microfilming. While the most advanced technology has been used to photograph and reproduce this document, the quality of the reproduction is heavily dependent upon the quality of the material submitted.

The following explanation of techniques is provided to help clarify markings or notations which may appear on this reproduction.

1. The sign or "target" for pages apparently lacking from the document photographed is "Missing Page(s)". If it was possible to obtain the missing page(s) or section, they are spliced into the film along with adjacent pages. This may have necessitated cutting through an image and duplicating adjacent pages to assure complete continuity.
2. When an image on the film is obliterated with a round black mark, it is an indication of either blurred copy because of movement during exposure, duplicate copy, or copyrighted materials that should not have been filmed. For blurred pages, a good image of the page can be found in the adjacent frame. If copyrighted materials were deleted, a target note will appear listing the pages in the adjacent frame.
3. When a map, drawing or chart, etc., is part of the material being photographed, a definite method of "sectioning" the material has been followed. It is customary to begin filming at the upper left hand corner of a large sheet and to continue from left to right in equal sections with small overlaps. If necessary, sectioning is continued again—beginning below the first row and continuing on until complete.
4. For illustrations that cannot be satisfactorily reproduced by xerographic means, photographic prints can be purchased at additional cost and inserted into your xerographic copy. These prints are available upon request from the Dissertations Customer Services Department.
5. Some pages in any document may have indistinct print. In all cases the best available copy has been filmed.

**University
Microfilms
International**

300 N. Zeeb Road
Ann Arbor, MI 48106



Order Number 1333611

Chromatic aberration of three-cylinder electrostatic lenses

Olson, David Fred, M.S.

The University of Arizona, 1988

U·M·I
300 N. Zeeb Rd.
Ann Arbor, MI 48106



PLEASE NOTE:

In all cases this material has been filmed in the best possible way from the available copy. Problems encountered with this document have been identified here with a check mark .

1. Glossy photographs or pages _____
2. Colored illustrations, paper or print _____
3. Photographs with dark background _____
4. Illustrations are poor copy _____
5. Pages with black marks, not original copy
6. Print shows through as there is text on both sides of page _____
7. Indistinct, broken or small print on several pages _____
8. Print exceeds margin requirements _____
9. Tightly bound copy with print lost in spine _____
10. Computer printout pages with indistinct print _____
11. Page(s) _____ lacking when material received, and not available from school or author.
12. Page(s) _____ seem to be missing in numbering only as text follows.
13. Two pages numbered _____. Text follows.
14. Curling and wrinkled pages _____
15. Dissertation contains pages with print at a slant, filmed as received _____
16. Other _____

U·M·I



CHROMATIC ABERRATION OF THREE-CYLINDER
ELECTROSTATIC LENSES

by

David Fred Olson

A Thesis Submitted to the Faculty of the
DEPARTMENT OF ELECTRICAL ENGINEERING

In Partial Fulfillment of the Requirements
For the Degree of

MASTER OF SCIENCE

In the Graduate College
THE UNIVERSITY OF ARIZONA

1 9 8 8

STATEMENT BY AUTHOR

This thesis has been submitted in partial fulfillment of requirements for an advanced degree at the University of Arizona and is deposited in the University Library to be made available to borrowers under rules of the Library.

Brief quotations from this thesis are allowable without special permission, provided that accurate acknowledgement of source is made. Requests for permission for extended quotation from or reproduction of this manuscript in whole or in part may be granted by the head of the major department or the Dean of the Graduate College when in his or her judgement the proposed use of the material is in the interest of scholarship. In all other instances, however, permission must be obtained from the author.

SIGNED: *D. F. Olson*

APPROVAL BY THESIS DIRECTOR

This thesis has been approved on the date shown below:

M. Szilagyi
M. Szilagyi
Professor of Electrical and
Computer Engineering

April 29, 1988
Date

ACKNOWLEDGEMENT

This work is supported by the National Science Foundation under Grant ECS 8700849.

TABLE OF CONTENTS

LIST OF ILLUSTRATIONS	5-6
ABSTRACT	7
INTRODUCTION	8
LENS GEOMETRY	8-9
METHOD OF CALCULATIONS	9-12
ACCURACY	12-13
RESULTS	13-17
REFERENCES	37

LIST OF ILLUSTRATIONS

FIG. 1. Schematics of the symmetric three-cylinder electrostatic lens.

FIG. 2. The chromatic aberration coefficient for infinite magnification C_{c0}/D as a function of the voltage ratio V_2/V_1 for $V_3/V_1=1.0$.

FIG. 3. The ratio of the chromatic aberration coefficient to the object-side focal length C_{c0}/f_0 as a function of the voltage ratio V_2/V_1 for $V_3/V_1=1.0$.

FIG. 4. The chromatic aberration coefficient for infinite magnification C_{c0}/D as a function of the voltage ratio V_2/V_1 for $V_3/V_1=5.0$.

FIG. 5. The ratio of the chromatic aberration coefficient to the object-side focal length C_{c0}/f_0 as a function of the voltage ratio V_2/V_1 for $V_3/V_1=5.0$.

FIG. 6. The chromatic aberration coefficient for infinite magnification C_{c0}/D as a function of the voltage ratio V_2/V_1 for $V_3/V_1=25.0$.

FIG. 7. The ratio of the chromatic aberration coefficient to the object-side focal length C_{c0}/f_0 as a function of the voltage ratio V_2/V_1 for $V_3/V_1=25.0$.

FIG. 8. The product of the magnification and the object-side chromatic aberration coefficient $|M|C_{c0}/D$ as a function of magnification $|M|$ for $A=0.5D$ and for the voltage ratio V_2/V_1 ranging from -0.6 to 0.7 with $V_3/V_1=1.0$.

FIG. 9. The product of the magnification and the object-side chromatic aberration coefficient $|M|C_{c0}/D$ as a function of magnification $|M|$ for $A=0.5D$ and for the voltage ratios V_2/V_1 ranging from 1.3 to 18.0 with $V_3/V_1=1.0$.

FIG.10. The product of the magnification and the object-side chromatic aberration coefficient $|M|C_{c0}/D$ as a function of magnification $|M|$ for $A=1.0D$ and for the voltage ratio V_2/V_1 ranging from 0.0 to 1.1 with $V_3/V_1=1.0$.

FIG.11. The product of the magnification and the object-side chromatic aberration coefficient $|M|C_{c0}/D$ as a function of magnification $|M|$ for $A=1.0D$ and for the voltage ratio V_2/V_1 ranging from 1.6 to 18.0 with $V_3/V_1=1.0$.

FIG.12. The product of the magnification and the object-side chromatic aberration coefficient $|M|C_{CO}/D$ as a function of magnification $|M|$ for $A=0.5D$ and for the voltage ratio V_2/V_1 ranging from -1.2 to 2.5 with $V_3/V_1=5.0$.

FIG.13. The product of the magnification and the object-side chromatic aberration coefficient $|M|C_{CO}/D$ as a function of magnification $|M|$ for $A=0.5D$ and for the voltage ratio V_2/V_1 ranging from 3.0 to 14.0 with $V_3/V_1=5.0$.

FIG.14. The product of the magnification and the object-side chromatic aberration coefficient $|M|C_{CO}/D$ as a function of magnification $|M|$ for $A=1.0D$ and for the voltage ratio V_2/V_1 ranging from 0.0 to 2.5 with $V_3/V_1=5.0$.

FIG.15. The product of the magnification and the object-side chromatic aberration coefficient $|M|C_{CO}/D$ as a function of magnification $|M|$ for $A=1.0D$ and for the voltage ratio V_2/V_1 ranging from 3.0 to 25.0 with $V_3/V_1=5.0$.

FIG.16. The product of the magnification and the object-side chromatic aberration coefficient $|M|C_{CO}/D$ as a function of magnification $|M|$ for $A=0.5D$ and for the voltage ratio V_2/V_1 ranging from -2.6 to 10.0 with $V_3/V_1=25.0$.

FIG.17. The product of the magnification and the object-side chromatic aberration coefficient $|M|C_{CO}/D$ as a function of magnification $|M|$ for $A=0.5D$ and for the voltage ratio V_2/V_1 ranging from 12.0 to 40.0 with $V_3/V_1=25.0$.

FIG.18. The product of the magnification and the object-side chromatic aberration coefficient $|M|C_{CO}/D$ as a function of magnification $|M|$ for $A=1.0D$ and for the voltage ratio V_2/V_1 ranging from 0.2 to 8.0 with $V_3/V_1=25.0$.

FIG.19. The product of the magnification and the object-side chromatic aberration coefficient $|M|C_{CO}/D$ as a function of magnification $|M|$ for $A=1.0D$ and for the voltage ratio V_2/V_1 ranging from 10.0 to 30.0 with $V_3/V_1=25.0$.

FIG.20. The chromatic aberration coefficient C_{CO}/D for the case $V_3/V_1=5.0$ and $V_2/V_1=0.9$ with $A/D=1.0$ and $|M|$ ranging from 0.01 to 100.0 .

ABSTRACT

Accurate calculations of the axial chromatic aberration coefficients of geometrically symmetric three-cylinder tripotential electrostatic lenses are presented for two different center electrode lengths. This is an extension of the first-order properties and the third-order spherical aberration coefficients published by Harting and Read.

INTRODUCTION

Three-cylinder electrostatic lenses for focusing charged particles have received considerable attention because of their simplicity and flexibility. Accurate and extensive data have been published on their first-order properties and spherical aberration coefficients. In order to more completely estimate the performance of a lens in an electron or ion optical system, however, the chromatic aberration must also be considered. The effect of chromatic aberration is especially important for focused ion beams produced by liquid metal ion sources. Very little has been published on this matter in the literature. The purpose of this paper is to extend the first-order properties (focal lengths and principal planes) and the third-order asymptotic spherical aberration coefficients of axially symmetric thin-walled three-cylinder electrostatic lenses presented by Harting and Read with data on their asymptotic axial chromatic aberration coefficients.

I. LENS GEOMETRY

The lens geometry of the three-electrode cylindrical lenses treated in this paper is identical to those of Harting and Read and is shown in Figure 1. All of the lens parameters are given in terms of the fundamental unit of

length D which is the diameter of the lens. The reference plane is considered to pass through the geometric center of the lens perpendicular to the optical axis. The two gaps separating the three electrodes are both equal to a distance $G = 0.1D$ and the distance A from the center of one gap to the center of the other is $0.5D$ for the first group of lenses and $1.0D$ for the second group. The ends of the outer cylinders are terminated by 60° -degree cones (not shown) with their bases at distances $5D$ from the reference plane and their apexes on the axis. Since the properties of the lens are only dependent on the electrode potential ratios, the voltage V_1 at the object side will remain the unit potential while the center electrode potential V_2 and the image-side electrode potential V_3 are varied as described in section II.

II METHOD OF CALCULATIONS

To obtain the optical properties of each cylindrical lens the axial potential must first be found. The charge-density method ⁽⁹⁾ has been used to solve Laplace's equation which produced the axial potential for the given lens geometry and applied potentials.

The charge-density program was run on a VAX 11/750 computer with a UNIX operating system in double precision. 560 axial mesh points were used for each run with a maximum

absolute error allowed to be less than $0.001V$. Since the charge density program takes a large computing time for each run, scaling transformations were used to facilitate analysis. Two different scaling transformations were used to obtain more accurate data:

1. $(v_1, v_2, v_3) = (-1V, 0V, +1V)$ and $(v_1, v_2, v_3) = (+1V, 0V, +1V)$ represent the first set of electrode voltage inputs to the charge-density program producing the axial scaling potential distributions P_{11} and P_{12} , respectively. The axial potential distribution $U(z)$ for each voltage set (V_1, V_2, V_3) is then given in volts as a function of P_{11} and P_{12} by

$$U(z) = V_2 + (V_3 - V_1)P_{11}(z)/2 + (V_1 + V_3 - 2V_2)P_{12}(z)/2 \quad (1)$$

2. $(v_1, v_2, v_3) = (1V, 0V, 0V)$, $(v_1, v_2, v_3) = (0V, 1V, 0V)$ and $(v_1, v_2, v_3) = (0V, 0V, 1V)$ represent the second set of electrode voltage inputs producing the distributions P_{21} , P_{22} and P_{23} , respectively. The axial potential distribution for each voltage set is now given by

$$U(z) = V_1P_{21} + V_2P_{22} + V_3P_{23} \quad (2)$$

After scaling for the given ratios $(1, V_2/V_1, V_3/V_1)$ and obtaining the axial potential distribution $U(z)$, the length of the lens was determined. It is defined as the length of the region bounded by field-free spaces on both sides. For

a field-free space $dU(z)/dz=0$, so our data were edited to exclude regions outside the points where $dU(z)/dz$ had just reached zero and remained essentially zero thereafter.

(10)

Munro's ray tracing program was then used to find the object-side chromatic aberration coefficients which can be expressed as second-degree polynomials in $1/M$ as follows:

$$C_{CO} = C_{CO0} + C_{CO1}(1/M) + C_{CO2}(1/M)^2 \quad (3)$$

C_{CO0} , C_{CO1} and C_{CO2} are the asymptotic chromatic aberration coefficients of expansion and M is the lens's magnification. Note that C_{CO0} is equivalent to the chromatic aberration coefficient for infinite magnification (C_{CO}) and C_{CO2} is related to the image-side coefficient for zero magnification $C_{Ci}(M=0)$ as follows:

$$C_{CO2} = (V_1/V_3)^{1.5} C_{Ci}(M=0) \quad (4)$$

The first-order asymptotic optical properties and the object-side asymptotic third-order spherical aberration coefficients have been calculated in order to compare the results with those obtained by Harting and Read and check the results with the Helmholtz-Lagrange relationship $(f_o/f_i) = (V_1/V_3)^{0.5}$ where f_o and f_i are the object- and image-side focal lengths, respectively.

The image-side spherical and chromatic aberration coefficients can easily be obtained from the object-side aberration coefficients as follows:

(7)

$$\text{and } C_{Si} = C_{SO} M^4 (V_3/V_1)^{1.5} \quad (5)$$

$$C_{Ci} = C_{CO} M^2 (V_3/V_1)^{1.5} \quad (6)$$

They were computed directly by the procedure described above only for checking the accuracy.

The object-side aberration coefficients for retarding lenses $(V_3/V_1, V_2/V_1, 1)$ have also been computed but only for comparison with the following equations:

$$C_{SO}(1/M, V_3/V_1, V_2/V_1, 1) = C_{SO}(M, 1, V_2/V_1, V_3/V_1) M^4 (V_3/V_1)^{1.5} \quad (7)$$

and

$$C_{CO}(1/M, V_3/V_1, V_2/V_1, 1) = C_{CO}(M, 1, V_2/V_1, V_3/V_1) M^2 (V_3/V_1)^{1.5} \quad (8)$$

III ACCURACY

The optical properties generated as described above were compared with the tabulated values of data published by Harting and Read. The focal lengths f_o and f_i were within 3%, the principal planes H_o and H_i were within 5% (where 'o' refers to the object side and 'i' refers to the image side) and the five spherical aberration expansion coefficients were all within 5% of Harting and Read's data except for the end values of V_2/V_1 for a few of the tables where discrepancies of 6% to 10% were observed. This is consistent with Harting and Read who estimated the accuracy of their data being about 10% and also with the fact that the greatest errors occur at the highest and lowest values of

V_2/V_1 for each V_3/V_1 value (the end values of the tables). Also, for our data, the focal lengths agreed within 3% with the Lagrange-Helmholtz relationship.

The image-side chromatic aberration coefficient (C_{ci}) was computed as described in Section II for magnifications ranging from 0.01 to 100. These directly computed values agreed with the C_{ci} values computed using our C_{co} data (see Eqn. 6) within 5%.

IV. RESULTS

For each triple-element lens, as described in section I, the chromatic aberration coefficients ($C_{co0}/D, C_{co1}/D, C_{co2}/D$) were computed. In addition, the values of C_{co}/D and C_{co}/f_0 were plotted vs. V_2/V_1 for fixed values of V_3/V_1 . Figures 2, 4 and 6 show plots of C_{co}/D for $V_3/V_1=1.0, 5.0$ and 25.0 , respectively. Figures 3, 5 and 7 show plots of C_{co}/f_0 for $V_3/V_1=1.0, 5.0$ and 25.0 , respectively. For each value of V_3/V_1 , plots for $A/D=0.5$ and $A/D=1.0$ are given on the same graph for comparison. The results show that for $V_3/V_1 < 5$ lenses with the shorter center electrode ($A/D=0.5$) have lower values of C_{co}/D at low values of V_2/V_1 . As V_3/V_1 increases, minimum values of the chromatic aberration coefficient occur at growing values of V_2/V_1 . Also as V_3/V_1 increases the values of C_{co}/D and C_{co}/f_0 are shown to vary less over the range of V_2/V_1 with smoother plots

observed for lenses with the shorter center electrode ($A/D=0.5$). The results show that lenses with higher V_3/V_1 ratios not only have lower chromatic aberration coefficients for infinite magnification but provide greater stability with respect to voltage variations.

We also have computed the ratio $|M|C_{CO}/D$ as a function of the absolute value of the linear magnification ranging from $|M|=0.1$ to $|M|=10.0$. They are represented as log-log plots in Figures 8-19 for $V_3/V_1=1.0, 5.0$ and 25.0 . Here the data for the two center electrode lengths, $A/D=0.5$ and $A/D=1.0$ are plotted separately for clarity. For each V_3/V_1 value, curves of $|M|$ vs. $|M|C_{CO}/D$ are plotted over the range of V_2/V_1 given in the previous figures. For each case separate plots for low and high values of V_2/V_1 are given to show clearly the variance of $|M|C_{CO}/D$ with the center electrode voltage. For low values of V_2/V_1 , as given in Figures 8, 10, 12, 14, 16 and 18, $|M|C_{CO}/D$ will increase with increasing V_2/V_1 . For higher values of V_2/V_1 this trend reverses and $|M|C_{CO}/D$ will decrease with increasing V_2/V_1 as shown in figures 9, 11, 13, 15, 17 and 19. We also observe from the graphs that for a given ratio of V_3/V_1 the lower values of $|M|C_{CO}/D$ can be found for lenses with $A/D=1.0$.

The minimum value of $|M|C_{CO}/D$ for each voltage ratio occurs at some optimum value of magnification M_{opt} . The

value of $|M_{opt}|$ lies approximately between 0.6 and 1.0, and it decreases as V_3/V_1 increases, except for lenses for which $A/D=1.0$ and $V_3/V_1 < 10$ where $|M_{opt}|$ was observed between 1.0 and 2.0 for high values of V_2/V_1 . The calculated value of M_{opt} is given by the simple relationship⁽⁷⁾

$$M_{opt} = -(C_{CO2}/C_{CO0})^{0.5} \quad (9)$$

M_{opt} , calculated using our data, was found to agree with this formula within 0.05%. For einzel lenses ($V_3/V_1=1$) we have $C_{CO2}=C_{CO0}$ and $|M_{opt}|=1.0$.

Further C_{CO}/D was computed for absolute values of the linear magnification between 0.01 and 100 for the case of $V_3/V_1=5.0$, $V_2/V_1=0.9$, $A/D=1.0$. The dependence of C_{CO}/D on $|M|$ is shown in Figure 20. As to be expected, C_{CO}/D nears the expansion coefficient C_{CO0}/D as $|M|$ increases, and as $|M|$ decreases C_{CO}/D approaches infinity.

For each voltage ratio ($1, V_2/V_1, V_3/V_1$) the image-side optical properties as well as the optical properties for retarding lenses ($V_3/V_1, V_2/V_1, 1$) were computed from the axial potential files following the procedure of Section II. The data for these cases can be obtained easily from the object-side accelerating lens data, as given by equations 5-8. The object- and image-side chromatic aberration coefficients of an accelerating lens are equivalent to the image- and object-side values, respectively, of the corres-

ponding retarding lens with reciprocal magnification. The figure of merit C_{CO}/f_0 for retarding lenses is calculated with ease using equation 8 and the following relationship

$$f_i(1, V_2/V_1, V_3/V_1) = f_0(V_3/V_1, V_2/V_1, 1) \quad (10)$$

All image-side properties for accelerating lenses and the object- and image-side properties of retarding lenses can be deduced from the object-side properties of the respective accelerating lenses by using Eqs. 5-8.

We shall now make a comparison of the three-cylinder lens with the two-cylinder lens, as discussed in a previous paper, with respect to their chromatic aberration. (11)

For both the two- and three-cylinder lenses lower values of C_{CO}/D , C_{CO}/f_0 , and $|M|C_{CO}/D$ are obtained by increasing the image-side potential (V_2/V_1 for the two-cylinder system and V_3/V_1 for the three-cylinder system) with respect to the object-side potential. It is clear that for the two-cylinder system smaller gaps between the object- and image-side cylinders produce lower chromatic aberration values for each value of V_2/V_1 . For the three-cylinder system the chromatic aberration values are mainly dependent on V_2/V_1 for each value of V_3/V_1 with a lesser dependence on gap size and center electrode length.

It is evident that a two-cylinder system with $V_2/V_1 = V_x$ is approximately equivalent to a three-cylinder system with

$V_2/V_1=1$ and $V_3/V_1=V_x$. However, by increasing the value of V_2/V_1 up to a certain value in the three-cylinder system the results improve dramatically. For example, the two-cylinder system with $V_2/V_1=5.0$ has $C_{CO} / f_0=1.3$ and the three-cylinder system with $V_2/V_1=1.0$ and $V_3/V_1=5.0$ has $C_{CO} / f_0=1.3$. But with $V_2/V_1=40.0$ and $V_3/V_1=5.0$ we have $C_{CO} / f_0=0.23$. A value of $C_{CO} / f_0 < 0.3$ for the two-cylinder system studied requires a value of $V_2/V_1 > 100.0$. Similar results hold for C_{CO} / D and $|M|C_{CO}/D$. Thus, for the three-cylinder lens lower chromatic aberration values are possible at lower potentials than for the two-cylinder lens. The three-cylinder system is also more versatile than the two-cylinder lens.

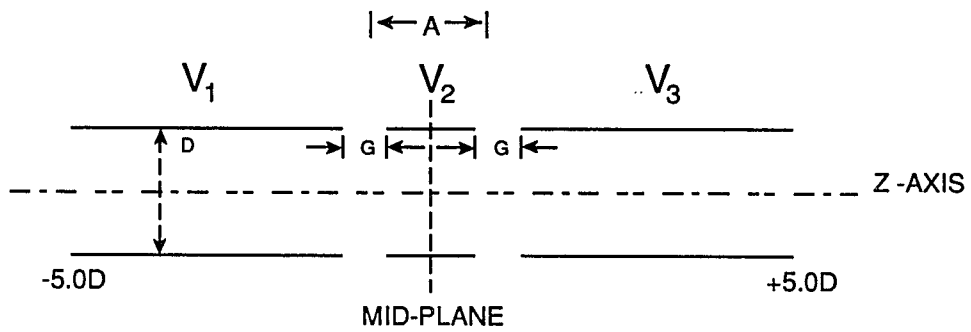


FIG. 1. Schematics of the symmetric three-cylinder electrostatic lens.

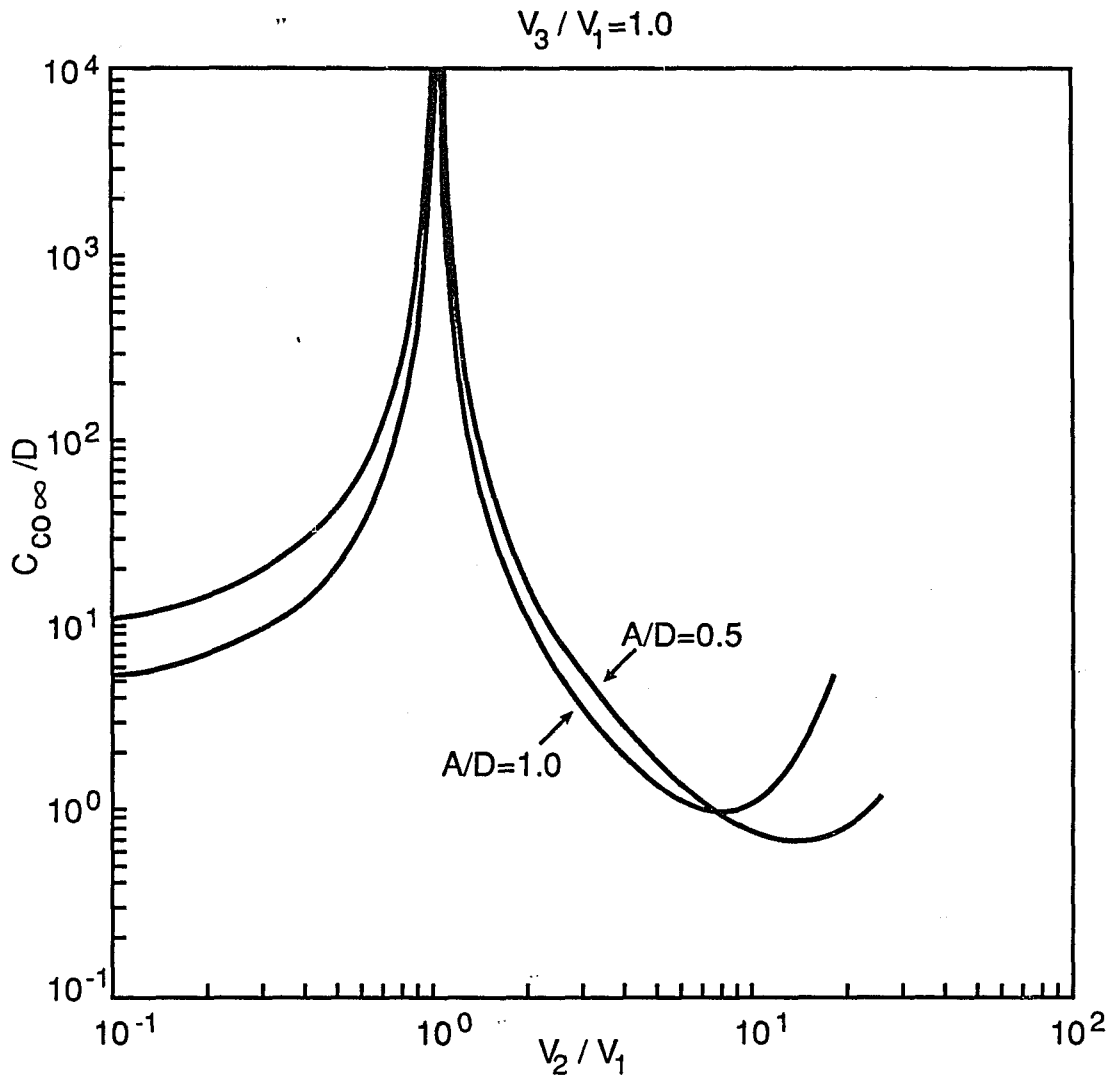


FIG. 2. The chromatic aberration coefficient for infinite magnification $C_{CO\infty}/D$ as a function of the voltage ratio V_2/V_1 for $V_3/V_1=1.0$.

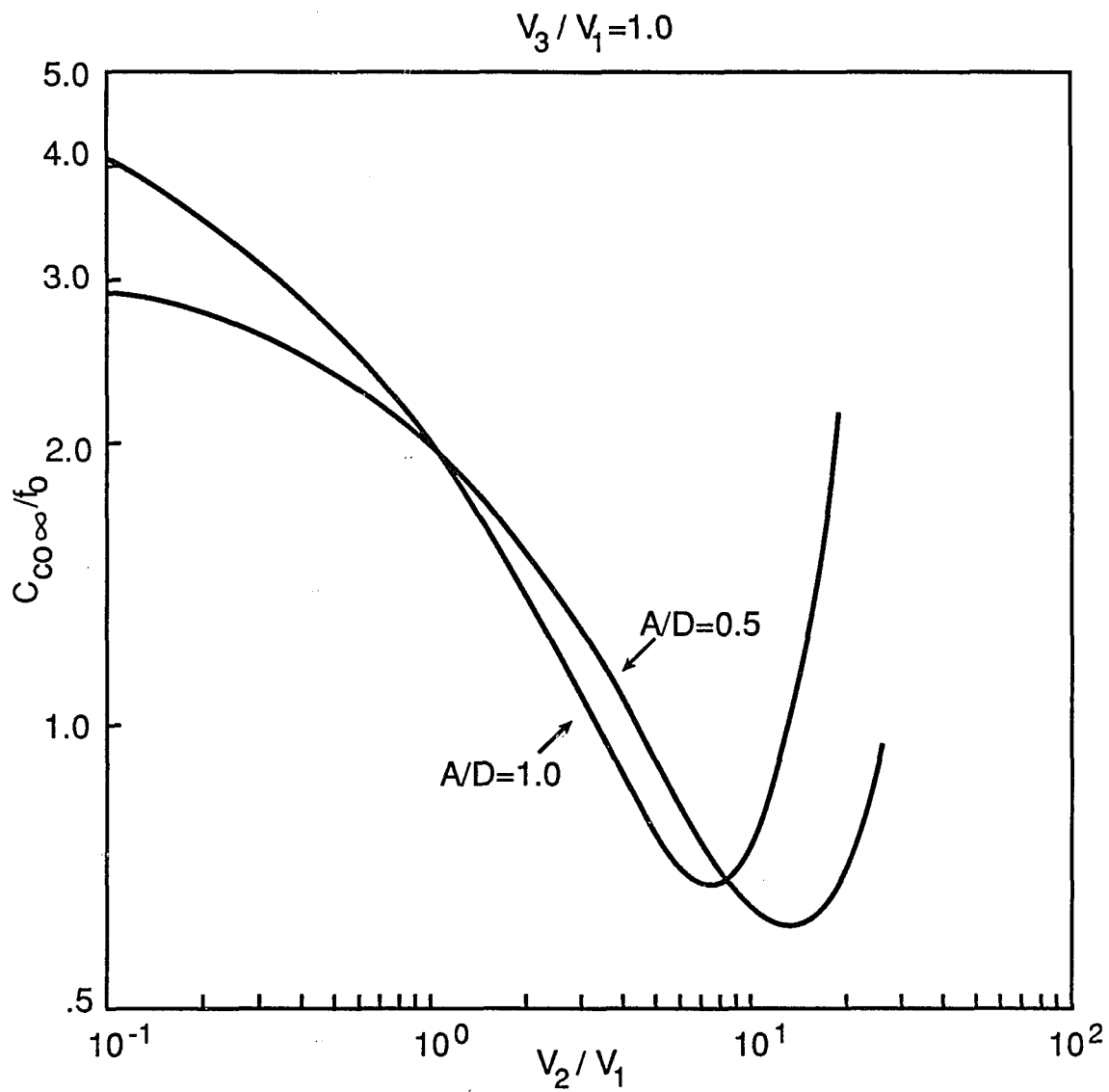


FIG. 3. The ratio of the chromatic aberration coefficient to the object-side focal length $C_{CO\infty}/f_0$ as a function of the voltage ratio V_2/V_1 for $V_3/V_1=1.0$.

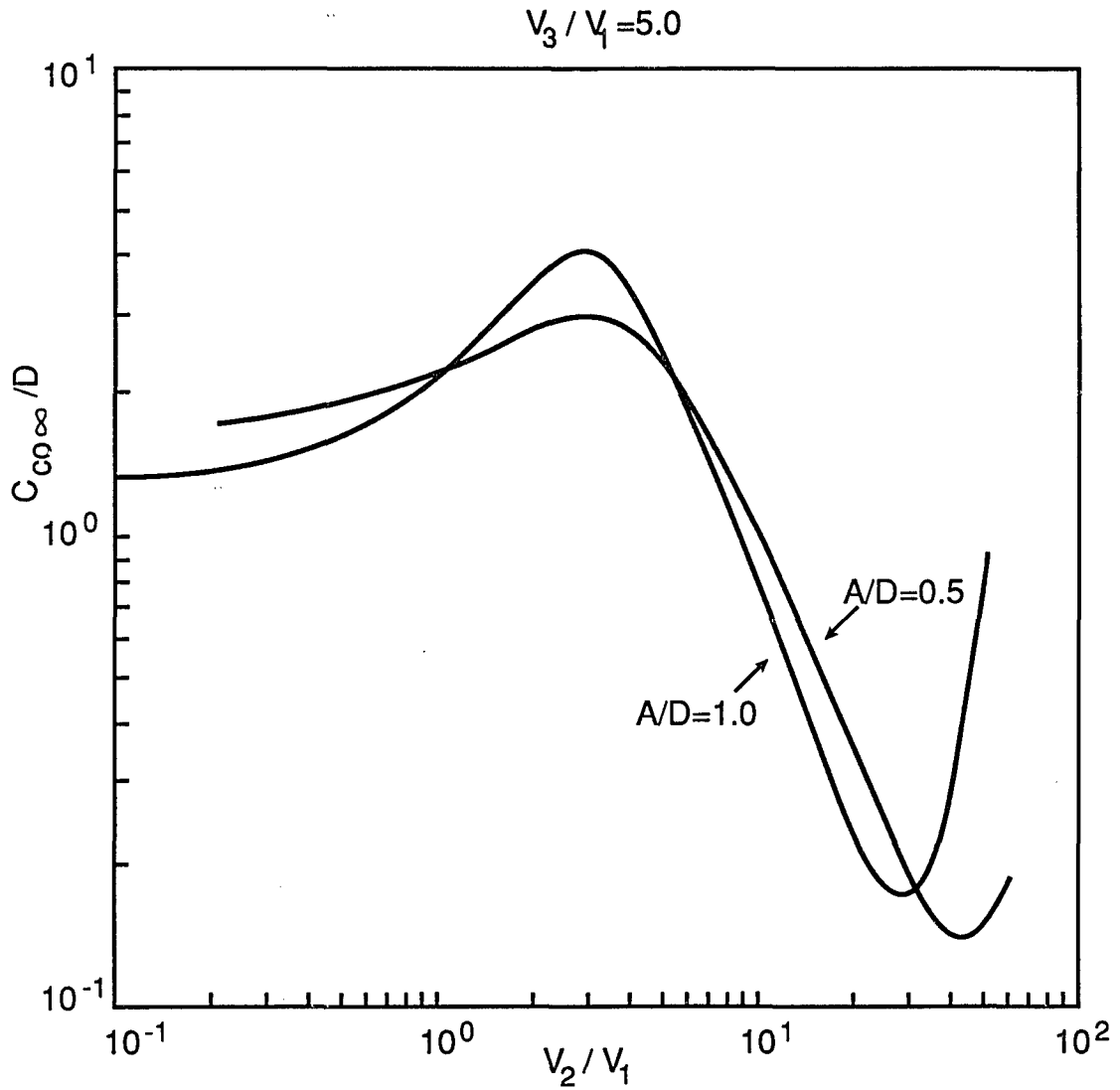


FIG. 4. The chromatic aberration coefficient for infinite magnification $C_{CO\infty}/D$ as a function of the voltage ratio V_2/V_1 for $V_3/V_1 = 5.0$.

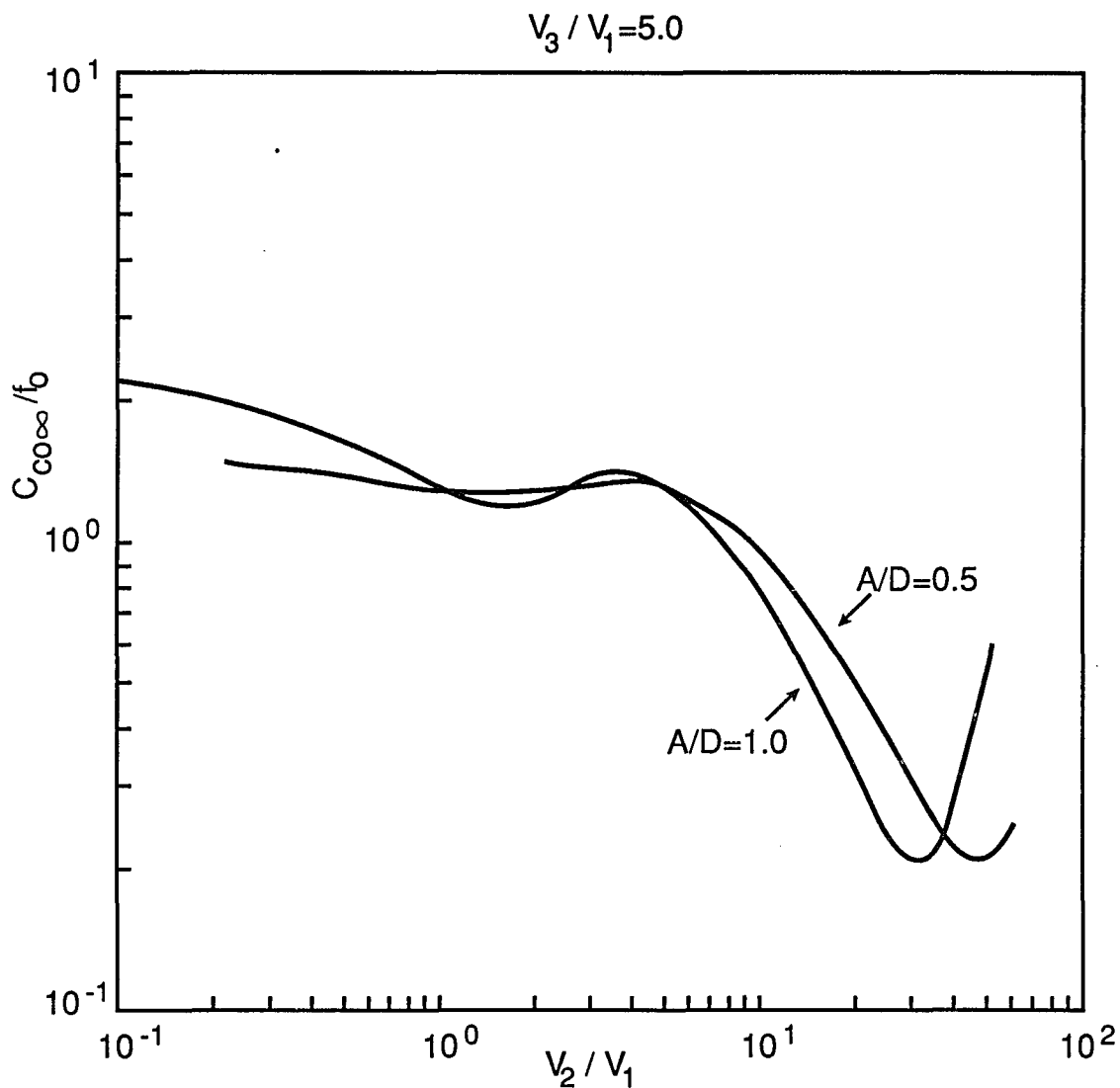


FIG. 5. The ratio of the chromatic aberration coefficient to the object-side focal length $C_{CO\infty}/f_0$ as a function of the voltage ratio V_2/V_1 for $V_3/V_1=5.0$.

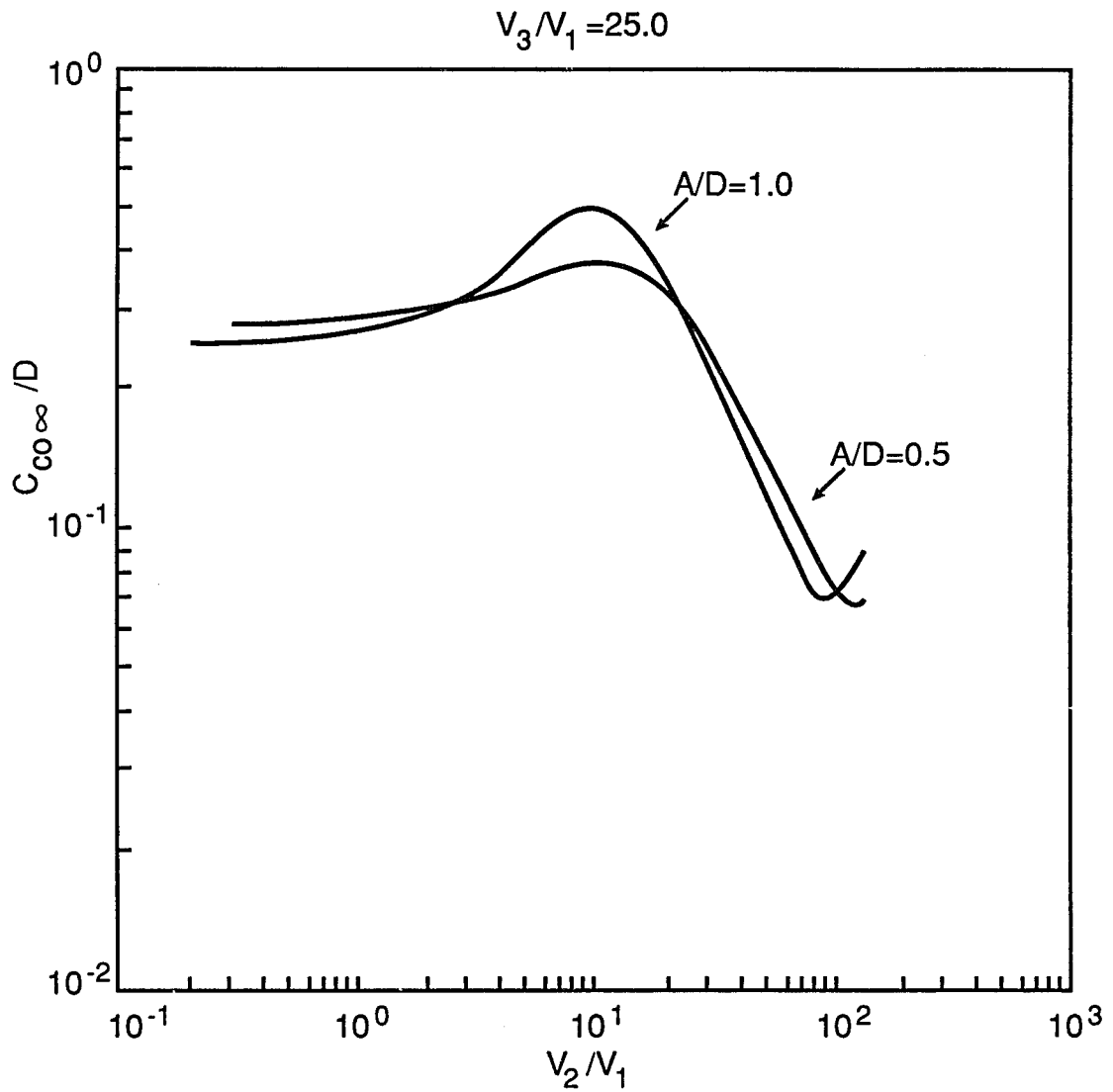


FIG. 6. The chromatic aberration coefficient for infinite magnification $C_{c0\infty}/D$ as a function of the voltage ratio V_2/V_1 for $V_3/V_1 = 25.0$.

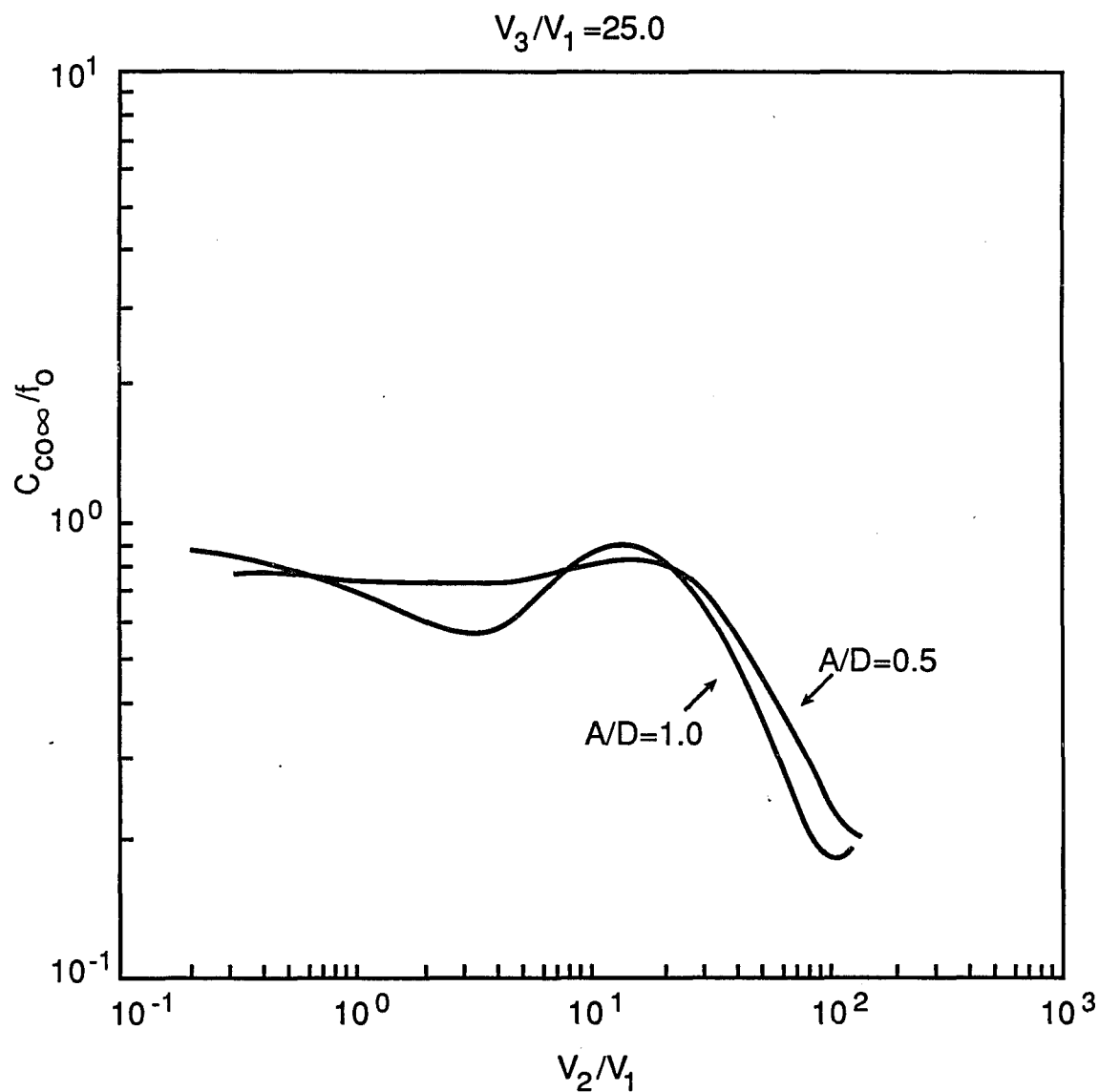


FIG. 7. The ratio of the chromatic aberration coefficient to the object-side focal length $C_{CO\infty}/f_0$ as a function of the voltage ratio V_2/V_1 for $V_3/V_1 = 25.0$.

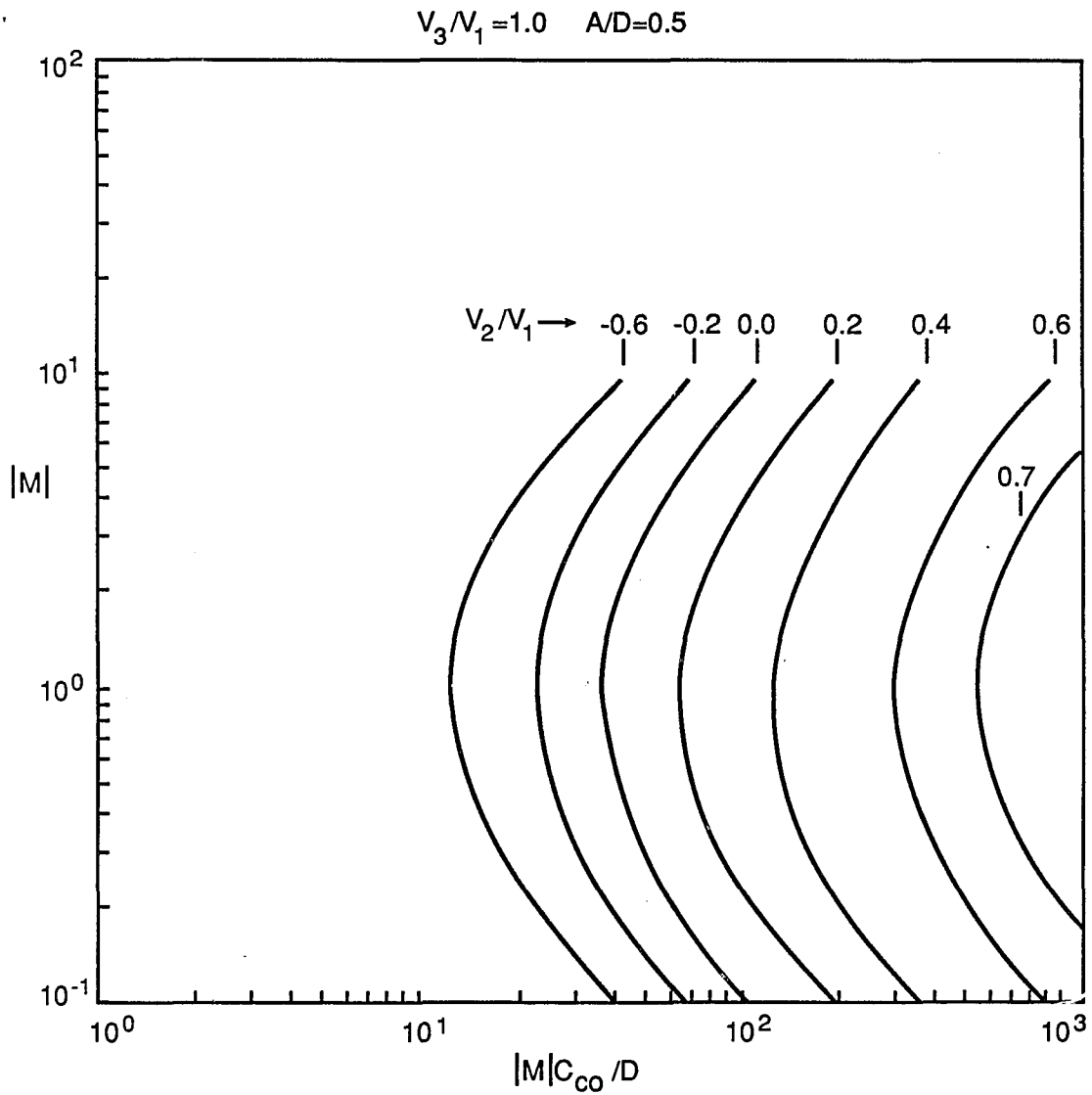


FIG. 8. The product of the magnification and the object-side chromatic aberration coefficient $|M|C_{co}/D$ as a function of magnification $|M|$ for $A=0.5D$ and for the voltage ratio V_2/V_1 ranging from -0.6 to 0.7 with $V_3/V_1=1.0$.

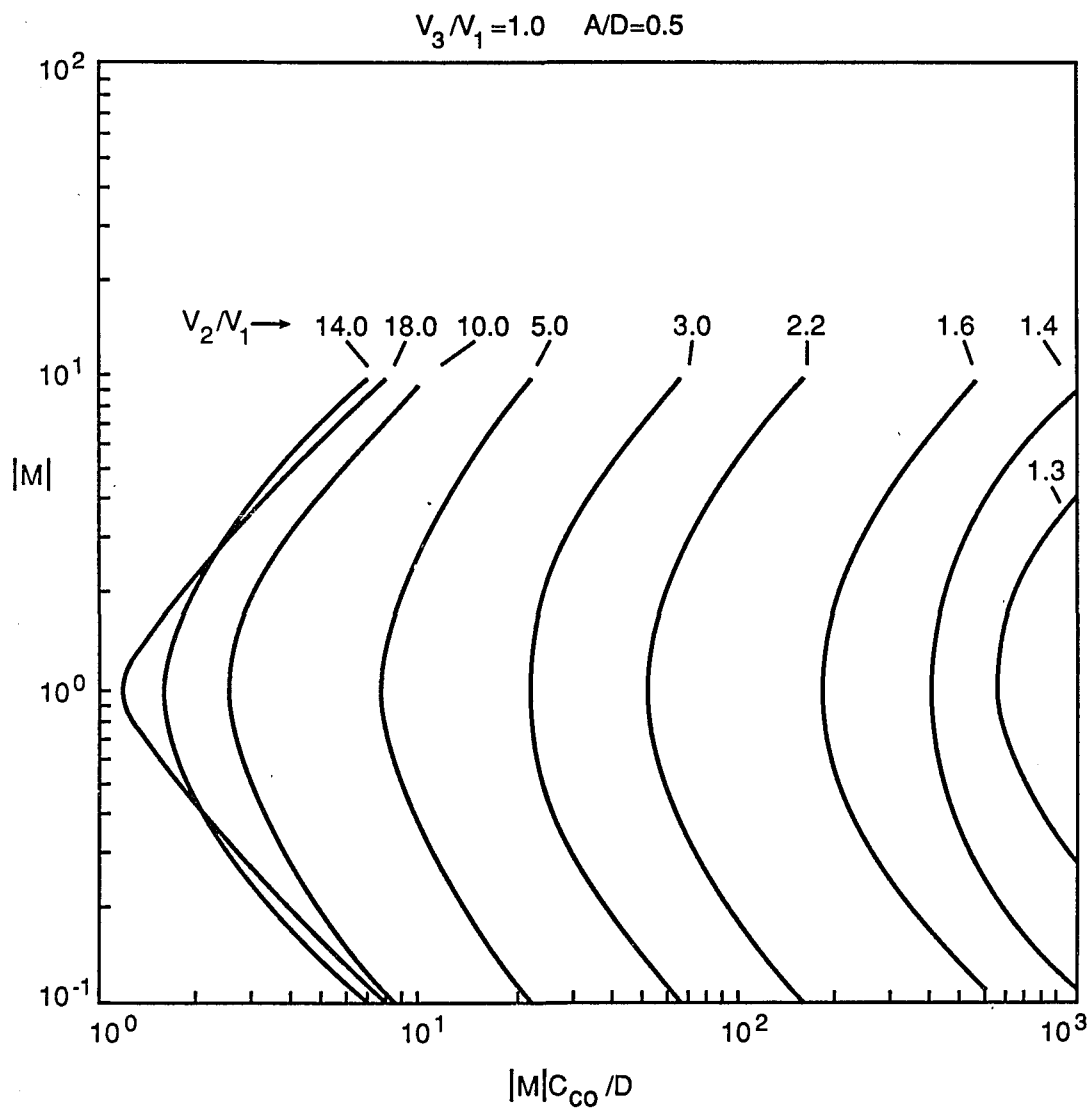


FIG. 9. The product of the magnification and the object-side chromatic aberration coefficient $|M|C_{CO}/D$ as a function of magnification $|M|$ for $A=0.5D$ and for the voltage ratios V_2/V_1 ranging from 1.3 to 18.0 with $V_3/V_1=1.0$.

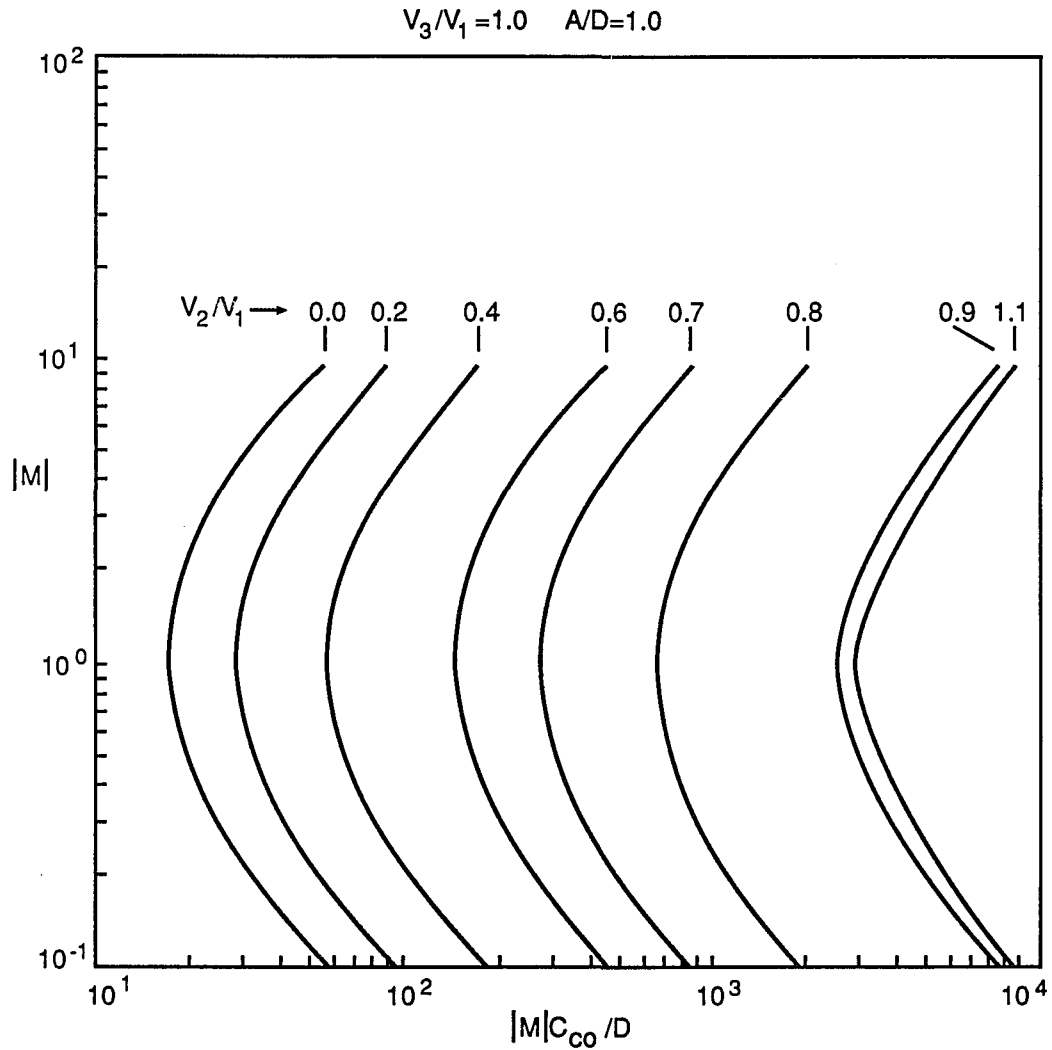


FIG.10. The product of the magnification and the object-side chromatic aberration coefficient $|M|C_{co}/D$ as a function of magnification $|M|$ for $A=1.0D$ and for the voltage ratio V_2/V_1 ranging from 0.0 to 1.1 with $V_3/V_1=1.0$.

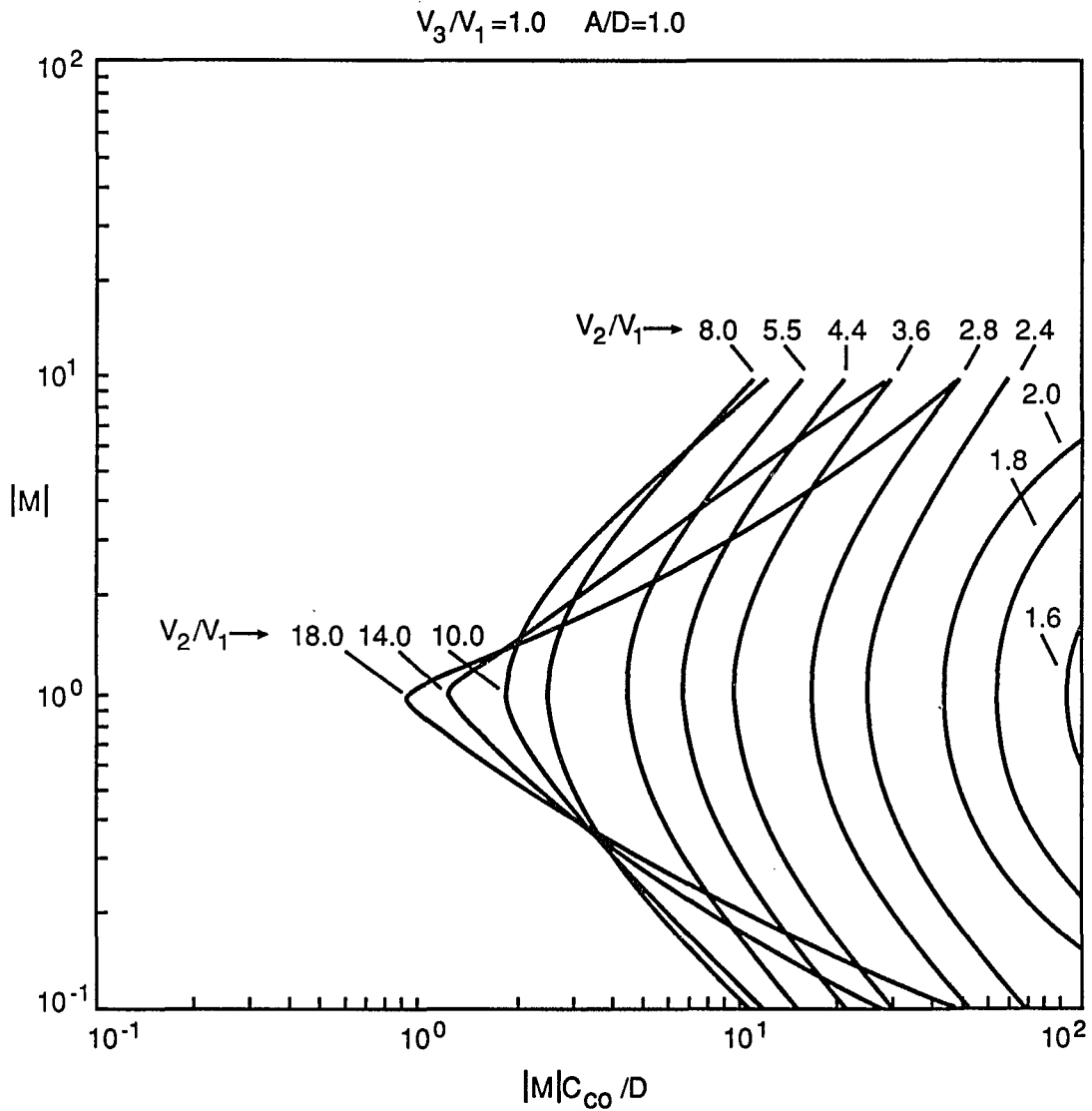


FIG.11. The product of the magnification and the object-side chromatic aberration coefficient $|M|C_{CO}/D$ as a function of magnification $|M|$ for $A=1.0D$ and for the voltage ratio V_2/V_1 ranging from 1.6 to 18.0 with $V_3/V_1=1.0$.

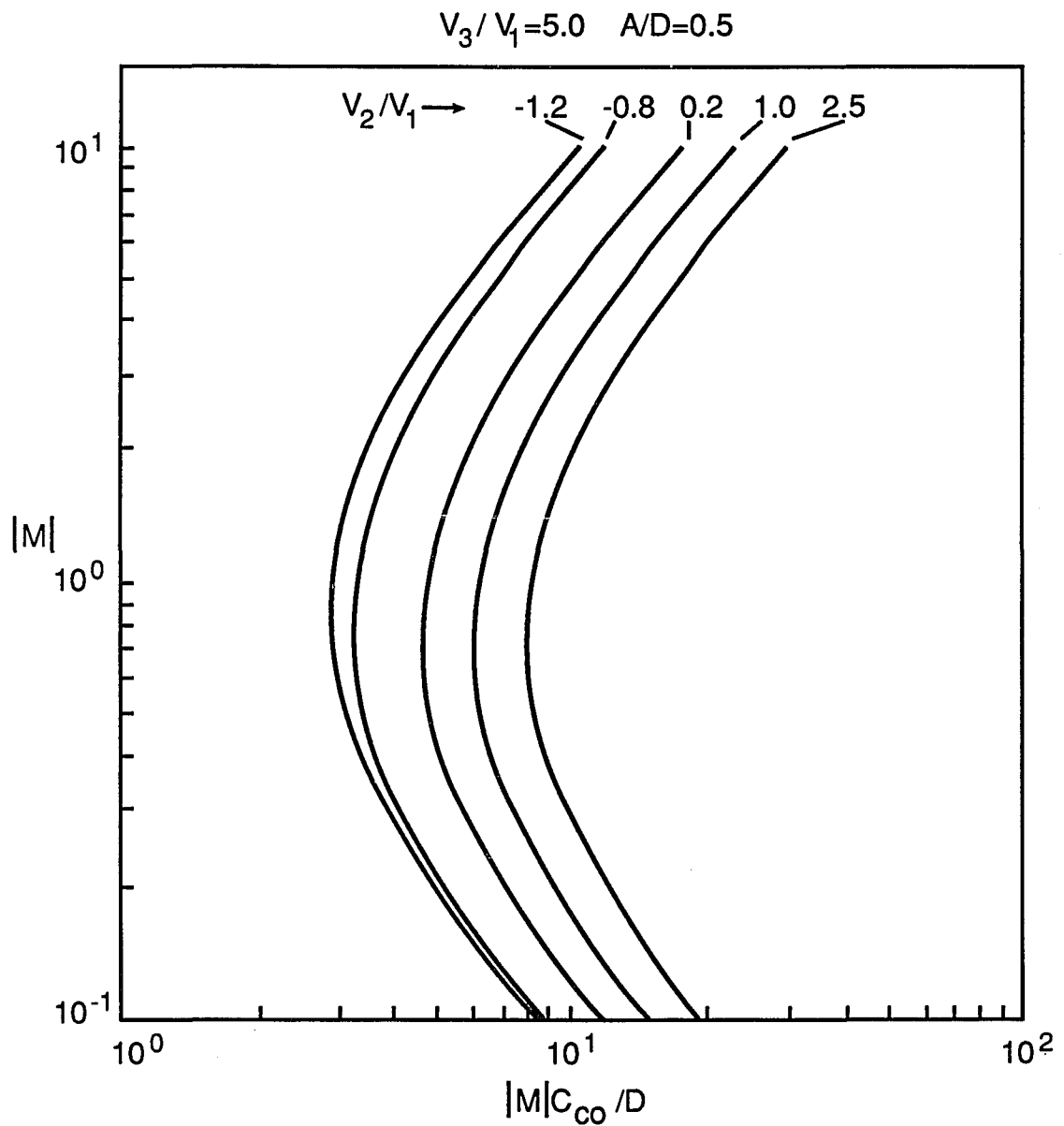


FIG.12. The product of the magnification and the object-side chromatic aberration coefficient $|M|C_{co}/D$ as a function of magnification $|M|$ for $A=0.5D$ and for the voltage ratio V_2/V_1 ranging from -1.2 to 2.5 with $V_3/V_1=5.0$.

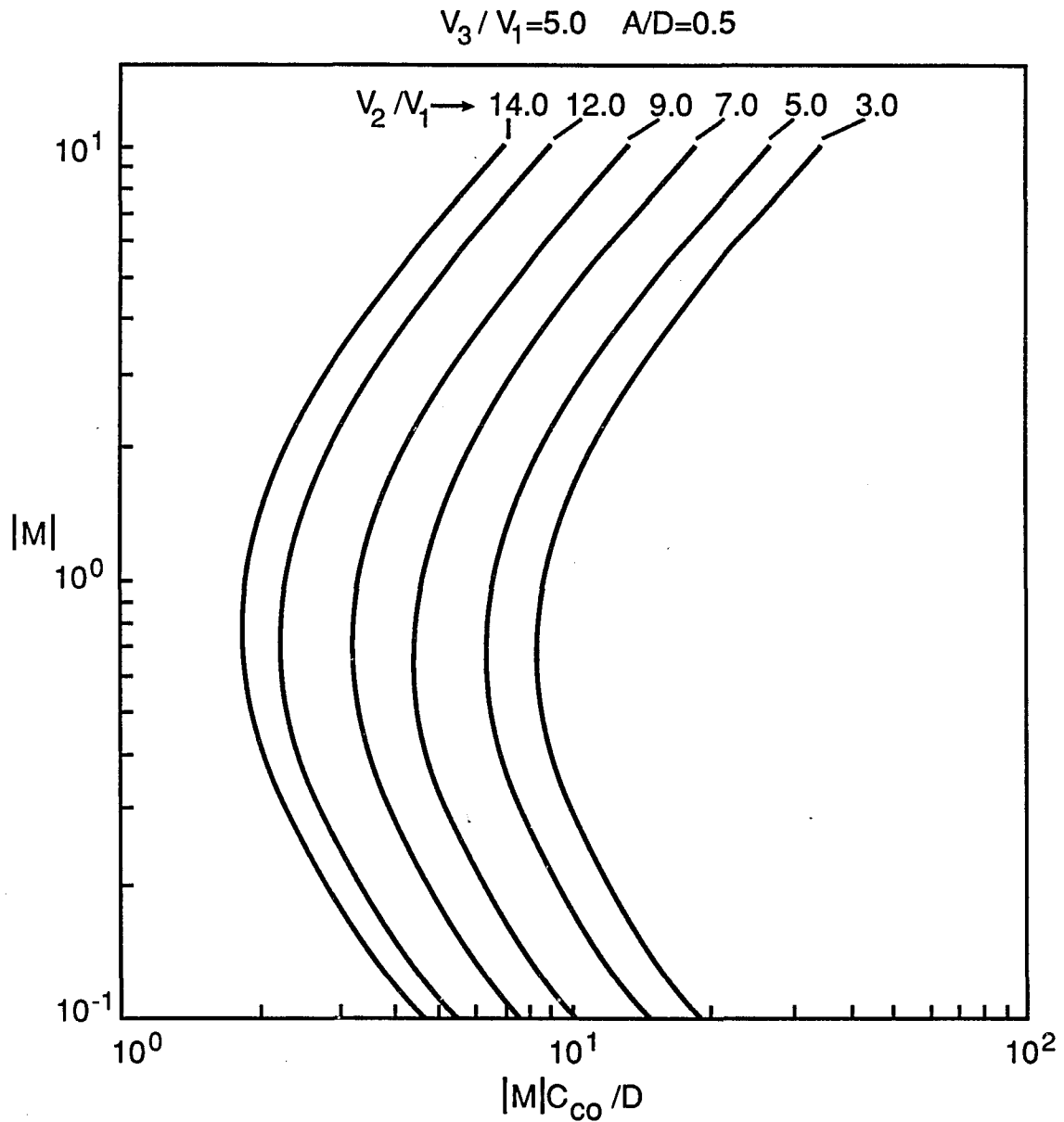


FIG.13. The product of the magnification and the object-side chromatic aberration coefficient $|M|C_{CO}/D$ as a function of magnification $|M|$ for $A=0.5D$ and for the voltage ratio V_2/V_1 ranging from 3.0 to 14.0 with $V_3/V_1=5.0$.

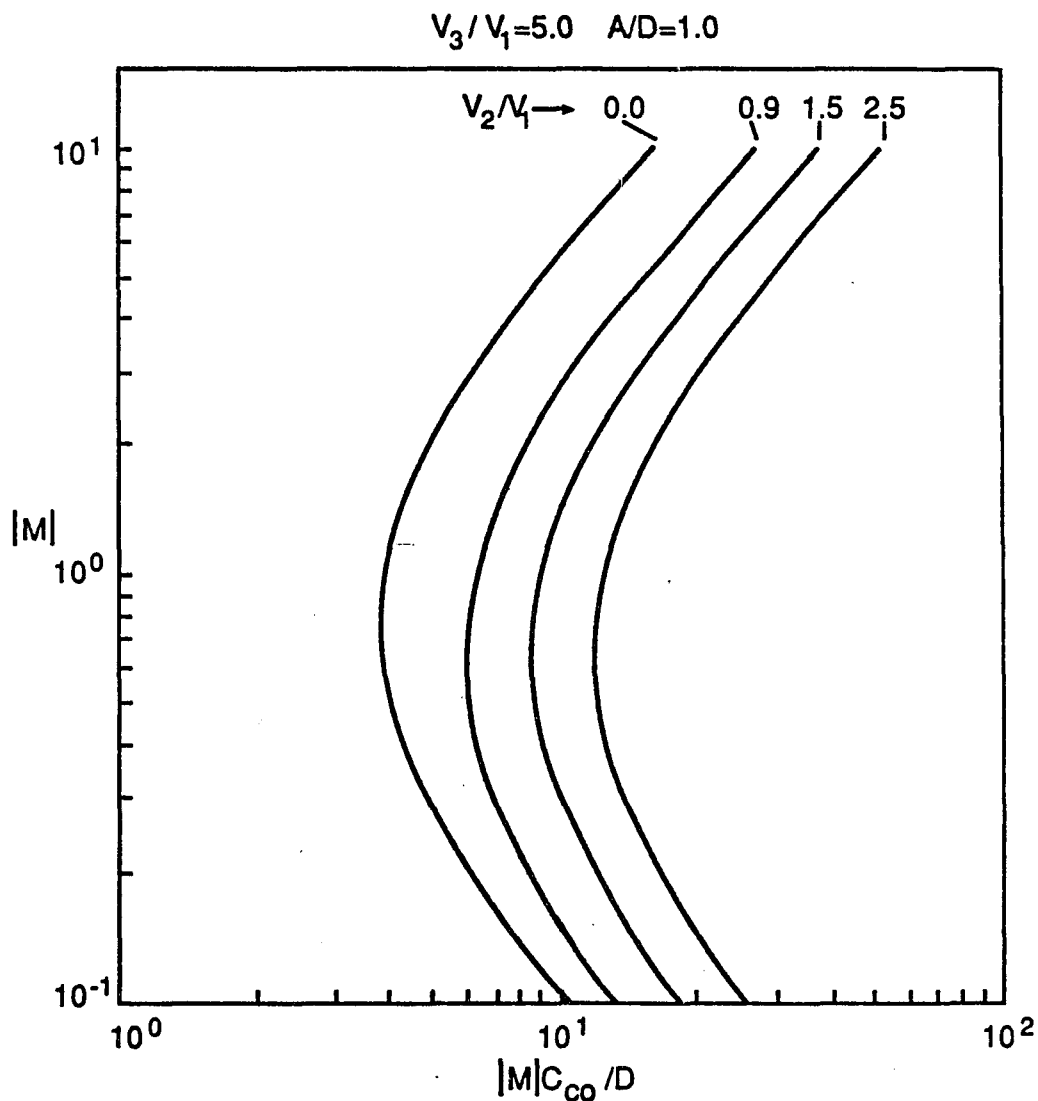


FIG.14. The product of the magnification and the object-side chromatic aberration coefficient $|M|C_{co}/D$ as a function of magnification $|M|$ for $A=1.0D$ and for the voltage ratio V_2/V_1 ranging from 0.0 to 2.5 with $V_3/V_1=5.0$.

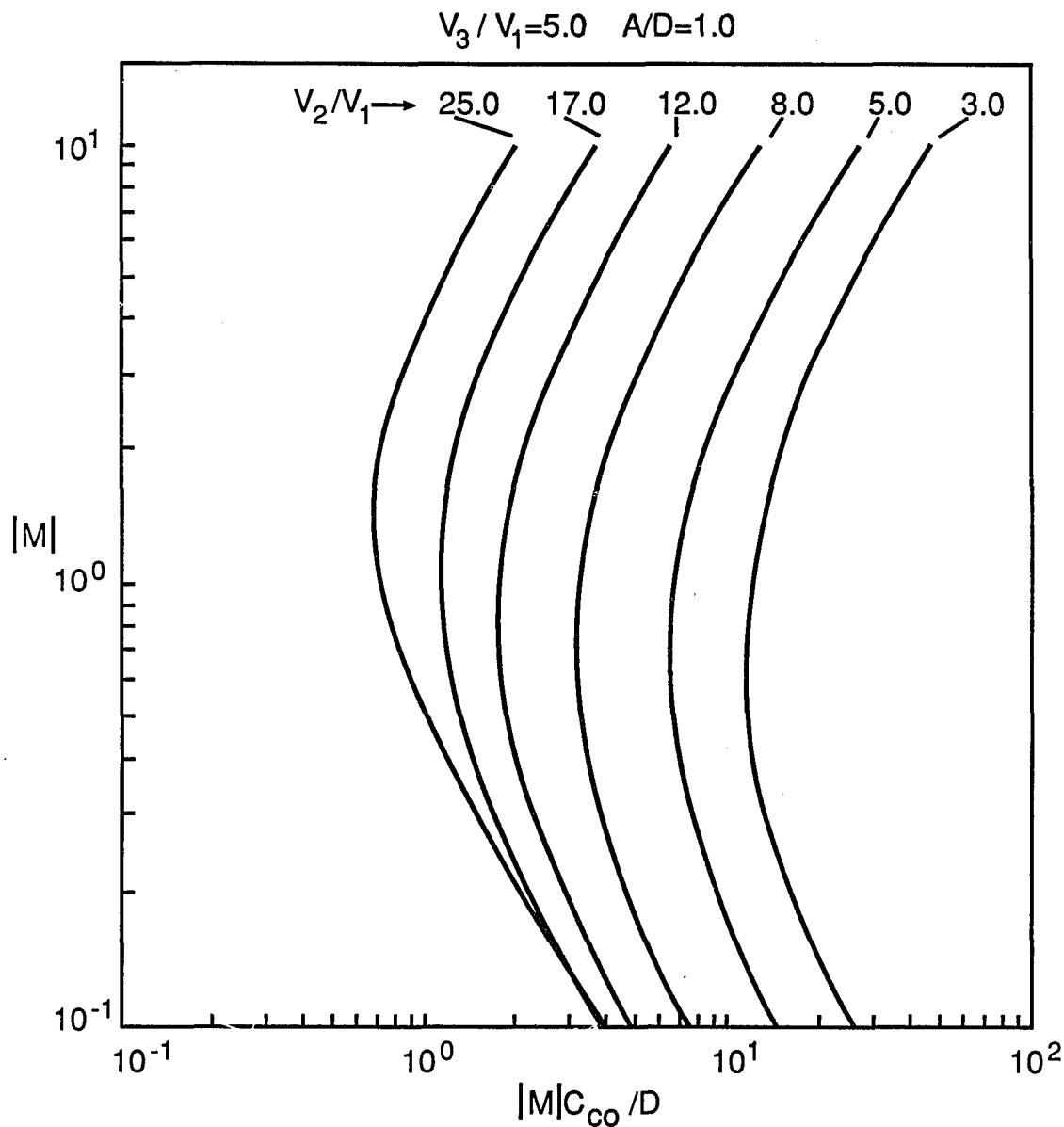


FIG.15. The product of the magnification and the object-side chromatic aberration coefficient $|M|C_{co}/D$ as a function of magnification $|M|$ for $A=1.0D$ and for the voltage ratio V_2/V_1 ranging from 3.0 to 25.0 with $V_3/V_1=5.0$.

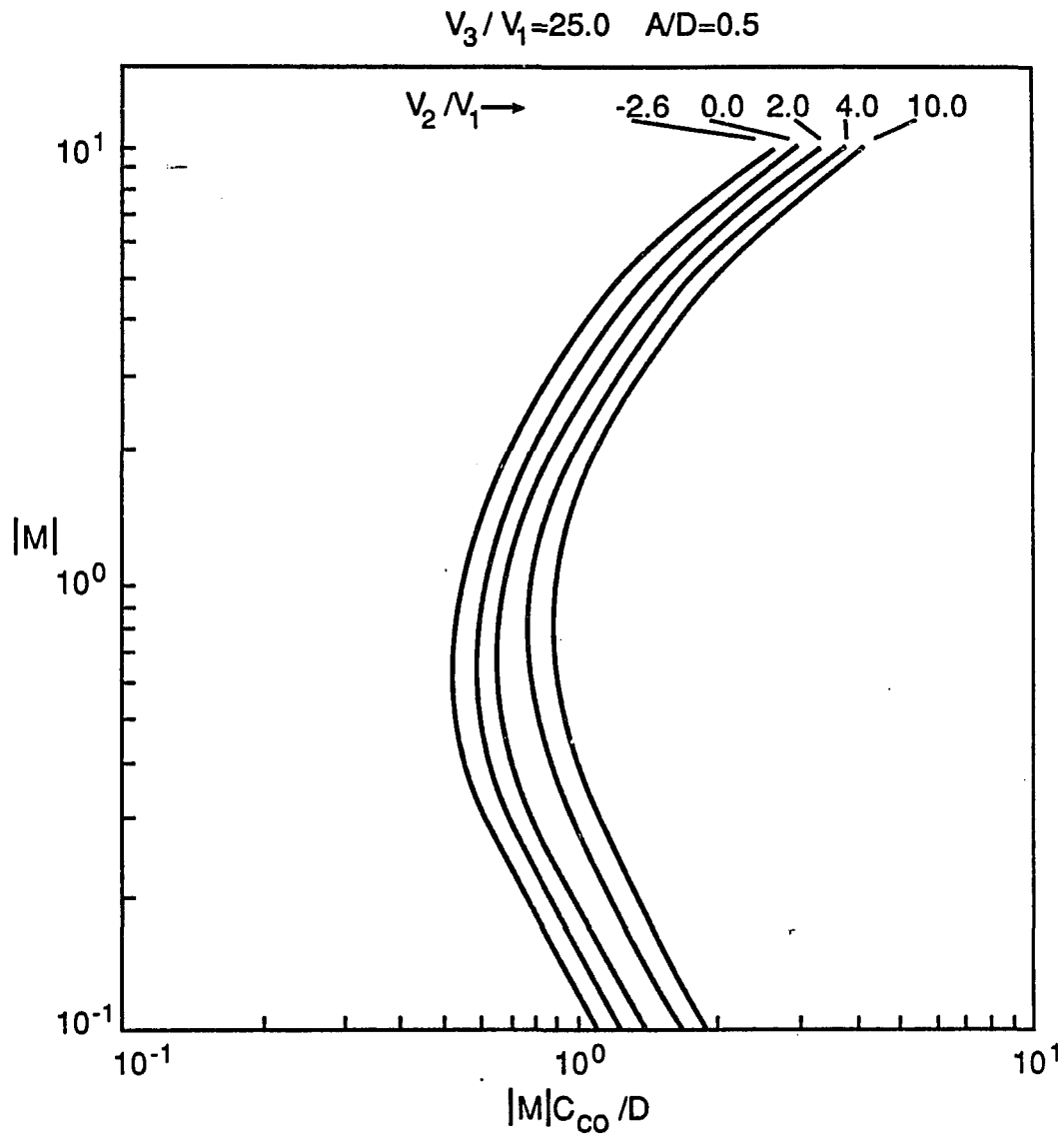


FIG.16. The product of the magnification and the object-side chromatic aberration coefficient $|M|C_{co}/D$ as a function of magnification $|M|$ for $A=0.5D$ and for the voltage ratio V_2/V_1 ranging from -2.6 to 10.0 with $V_3/V_1=25.0$.

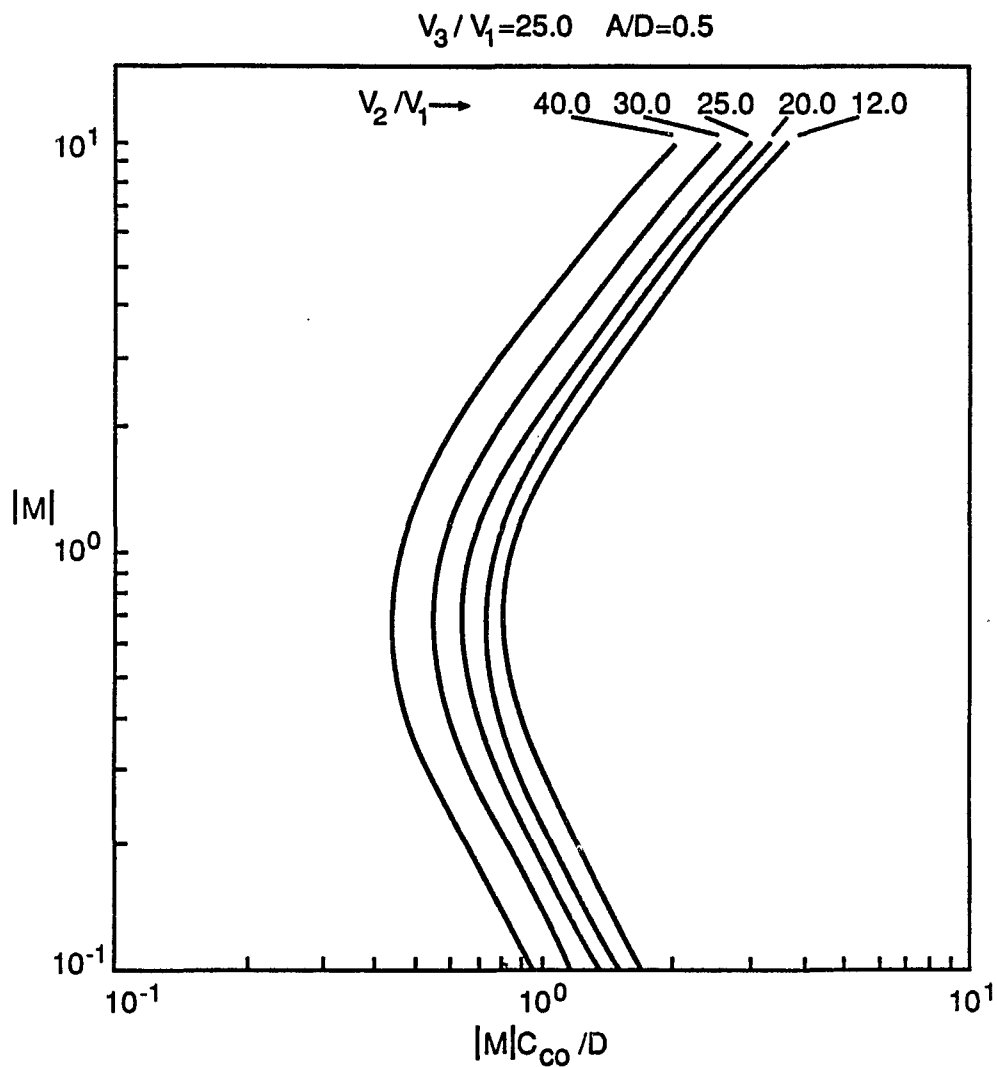


FIG.17. The product of the magnification and the object-side chromatic aberration coefficient $|M|C_{co}/D$ as a function of magnification $|M|$ for $A=0.5D$ and for the voltage ratio V_2/V_1 ranging from 12.0 to 40.0 with $V_3/V_1=25.0$.

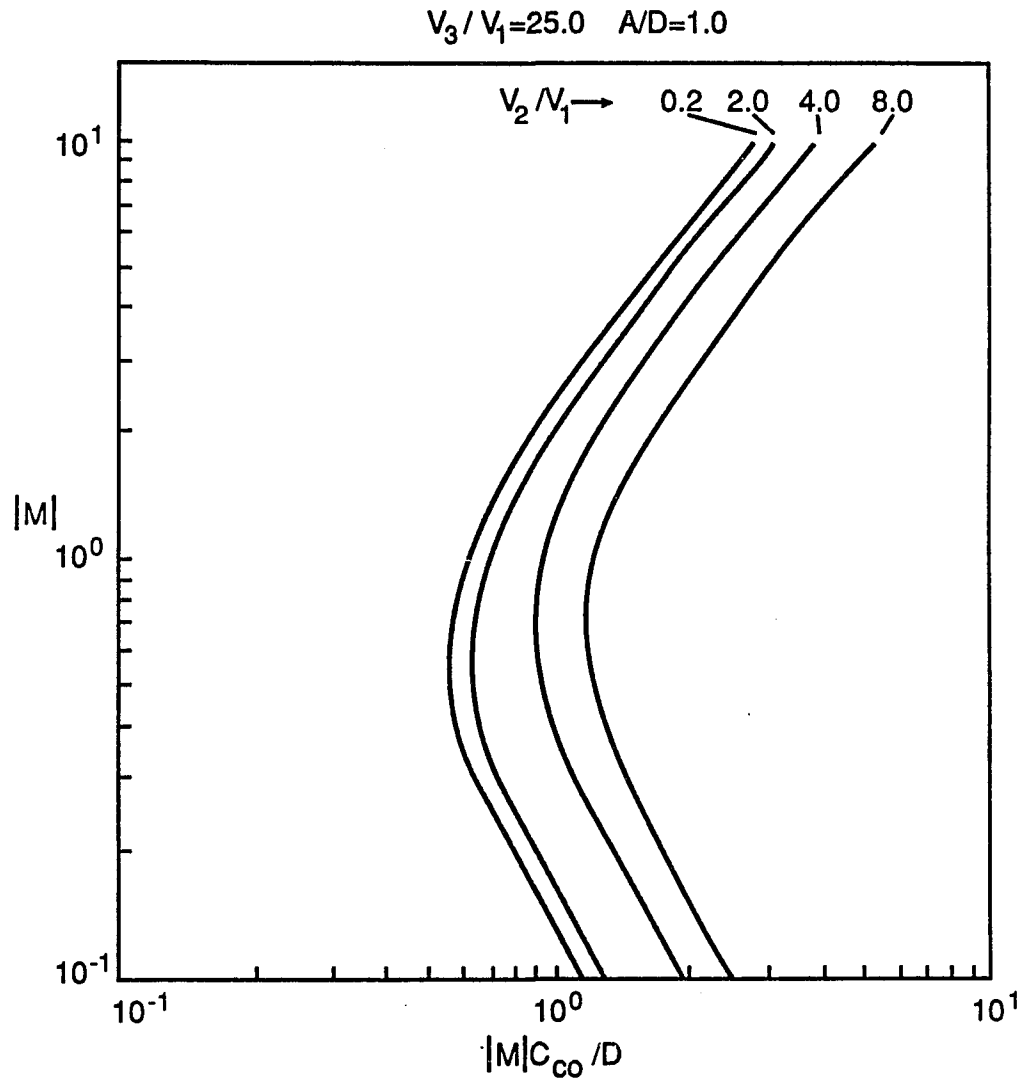


FIG.18. The product of the magnification and the object-side chromatic aberration coefficient $|M|C_{co}/D$ as a function of magnification $|M|$ for $A=1.0D$ and for the voltage ratio V_2/V_1 ranging from 0.2 to 8.0 with $V_3/V_1=25.0$.

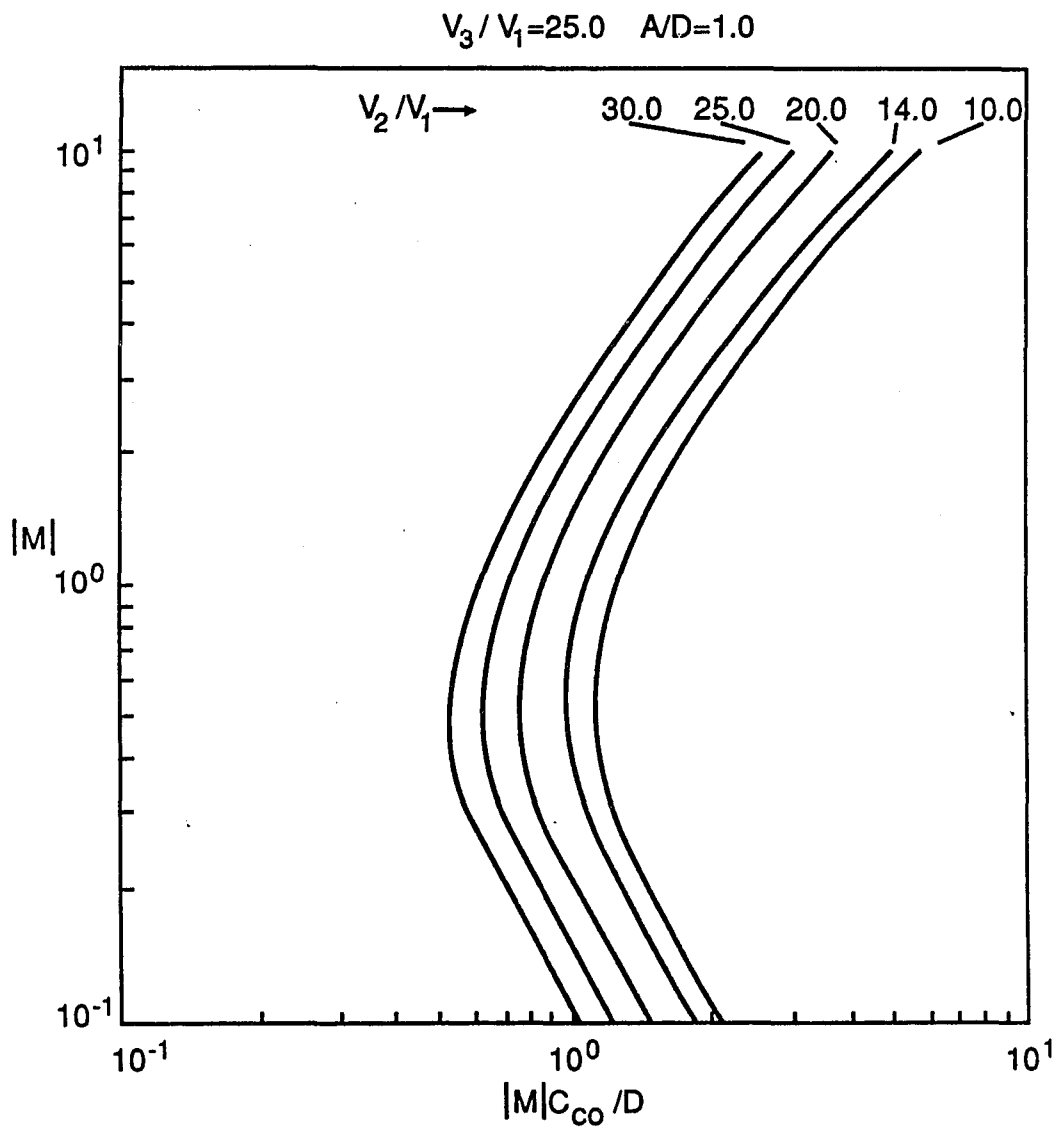


FIG.19. The product of the magnification and the object-side chromatic aberration coefficient $|M|C_{CO}/D$ as a function of magnification $|M|$ for $A=1.0D$ and for the voltage ratio V_2/V_1 ranging from 10.0 to 30.0 with $V_3/V_1=25.0$.

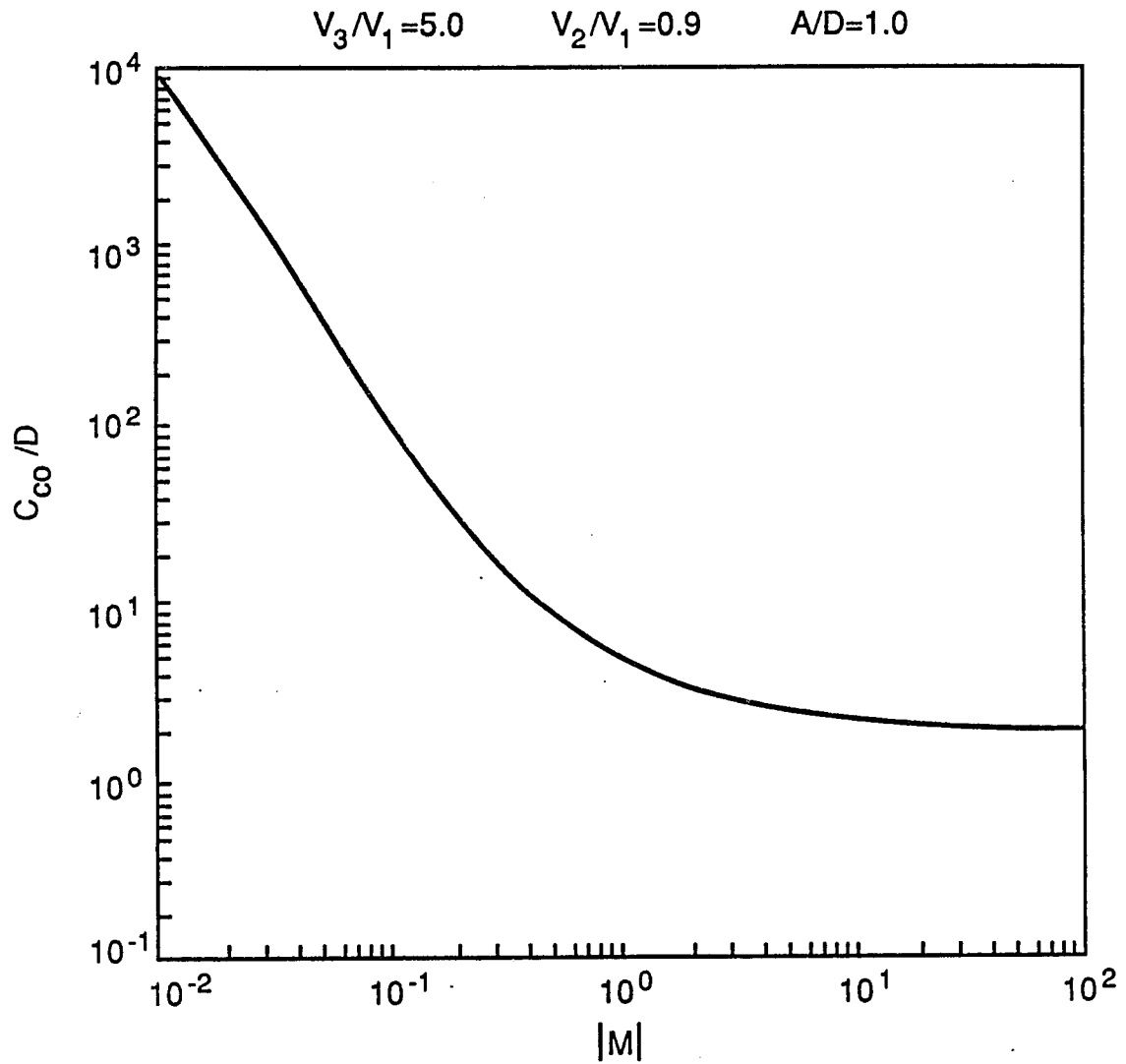


FIG.20. The chromatic aberration coefficient C_{co}/D for the case $V_3/V_1=5.0$ and $V_2/V_1=0.9$ with $A/D=1.0$ and $|M|$ ranging from 0.01 to 100.0 .

REFERENCES

1. E. Harting and F. H. Read, 'Electrostatic Lenses' (Elsevier, Amsterdam, Oxford, New York, 1976), pp.113-171.
2. A. B. El-Kareh and M. A. Sturans, J.Appl.Phys. 42(5), 1870-1876 (1971).
3. P. Bonjour, Rev. Phys. Appl. 14, 533-540, 715-728 (1979).
4. T. Saito and O. J. Sovers, J. Appl. Phys. 48(6), 2306-2311 (1977).
5. D. W. O. Heddle, N. Papadovassilakis and A. M. Yateem, J. Phys. E: Sci. Instrum. 15, 1210-1213 (1982).
6. M. Szilagyi and J. Szep, IEEE Transactions on Electron Devices, ED-34, 12, 2634-2642 (1987).
7. M. Szilagyi, Electron and Ion Optics (Plenum, New York, 1988).
8. A. Wagner, Solid-State Technol. 5, 97 (1983).
9. D. R. Cruise, J. Appl. Phys. 34, 12, 3477 (1963).
10. E. Munro, "A set of computer programs for calculating the properties of electron lenses", Cambridge Univ. Eng. Dept. Rept. CUED/B-ELECT/TR 45 (Cambridge Univ., England, 1975).
11. P. S. Vijayakumar and M. Szilagyi, Rev. Sci. Instrum. 58(6), 953-957 (1987).